Intramolecular Electron Transfer in Cytochrome *c* Oxidase: A Cascade of Equilibria†

Michael I. Verkhovsky,* Joel E. Morgan, and Mårten Wikström

Helsinki Bioenergetics Group, Department of Medical Chemistry, University of Helsinki, Siltavuorenpenger 10A, SF-00170, Helsinki, Finland

Received June 29, 1992; Revised Manuscript Received September 15, 1992

ABSTRACT: Intramolecular electron redistribution in cytochrome *c* oxidase after photolysis of the partially reduced CO-bound enzyme was followed at a number of different wavelengths by absorption spectroscopy. Spectra were constructed for the first two phases of this process. The first phase ($\tau = 3$ μs) has a spectrum essentially identical to the difference between the Fe_a and Fe_{a_3} reduced-minus-oxidized spectra, indicating a 1:1 stoichiometry between the amount of Fe_{a_3} oxidized and Fe_a reduced. It is not necessary to invoke reduction or oxidation of other redox carriers in this phase. The second phase ($\tau = 35$ μs) spectrum appears to be a linear combination of the Fe_{a_3} and Fe_a reduced-minus-oxidized difference spectra, reflecting the oxidation of four parts of Fe_{a_3} for every part of Fe_a oxidized. This process can be described in terms of transfer to Cu_A of electrons from the $Fe_{a_3} \leftrightarrow Fe_a$ equilibrium system established in the first phase. The relative contributions of Fe_{a_3} and Fe_a in the second phase allow us to calculate the equilibrium constant for $Fe_{a_3} \leftrightarrow Fe_a$ electron exchange, which yields a ΔE_m of 36 mV for the two centers (Fe_{a_3} more positive). Together with the apparent rate constant for the fast phase, this equilibrium constant yields, in turn, the forward (k_f) and reverse (k_r) rates for electron transfer from Fe_a to Fe_{a_3} as follows: $k_f = 2.4 \times 10^5$ s^{-1} and $k_r = 6 \times 10^4$ s^{-1}. k_f is much faster than any observed step in the reaction of the reduced enzyme with O_2. Thus, the catalytic mechanism of O_2 reduction to water is not rate-limited by electron transfer from Fe_a to the binuclear Fe_{a_3}/Cu_B site.

Cytochrome *c* oxidase contains four redox-active metal centers, two of which (Fe_{a_3} and Cu_B)[1] form a binuclear site, responsible for the catalysis of oxygen reduction, and two of which (Fe_a and Cu_A) serve to deliver electrons to the oxygen binding site from the respiratory chain. Binding CO in place of oxygen raises the redox potentials of Fe_{a_3} and Cu_B and makes it possible to prepare a mixed-valence compound of the enzyme in which the metals of the oxygen reduction site are reduced while the other carriers remain oxidized [see review by Wikström et al. (1981)]. Upon photolysis of CO, the E_m's of the binuclear site metals drop and electrons redistribute among all four metal centers, resulting in partial reduction of Fe_a and Cu_A. Observation of this electron "backflow" is one of the few direct methods by which intramolecular electron transfer in cytochrome *c* oxidase can be studied (Boelens et al., 1982; Brzezinski & Malmström, 1987; Morgan et al. 1989).

Oliveberg and Malmström (1991) were able to resolve two kinetic phases after CO photolysis, with rates of 2×10^5 and 1.3×10^4 s^{-1}. The first phase was assigned as oxidation of Fe_{a_3} accompanied by reduction of both Cu_B and Fe_a. More recently, however, Einarsdóttir et al. (1992) invoked oxidation of Cu_B to explain the appearance, in the first phase, of spectral features at 520 and 390 nm. The assignments in these two papers are clearly incompatible, since the former calls for reduction of Cu_B and the latter, its oxidation. There is general agreement that the second phase involves electron transfer from Fe_a to Cu_A (Morgan et al., 1989; Oliveberg & Malmström, 1991).

We have followed these processes at a number of wavelengths in order to determine the spectra of the two electron-transfer-related phases. On the basis of these spectra, we are able to make clear assignments as to the donor(s) and acceptor(s) in each phase.

MATERIALS AND METHODS

Bovine heart cytochrome *c* oxidase was prepared by a modification of the method of Hartzell and Beinert (1974). During enzyme preparation, the pH was kept above 7.8 (Baker et al., 1987). No ethanol was used to remove the Triton X-114 following the red/green cut; instead, the green pellet was repeatedly resuspended in the preparation buffer (without ethanol) and centrifuged until the amount of detergent was too small to cause the supernatant to bubble when shaken.

The enzyme was further purified at the time of sample preparation by ion-exchange chromatography on DEAE-Sepharose (DE-52, Whatman, or CL65, Pharmacia). Pasteur pipette sized columns were used. The columns were pre-equilibrated with a buffer containing 40 mM Tris, pH 7.4, and 0.5% Tween-80, and the same buffer was used for washing after the enzyme was loaded. The enzyme was eluted with a buffer containing 40 mM tris pH 7.4, 400 mM NaCl and 0.5% Tween-80, and this buffer was also used for dilution.

Routine vacuum-line procedures were used for sample preparation. Gases in the sample were exchanged by a washing/dilution procedure in which the gas in the cuvette headspace was replaced and then the liquid sample was gently mixed, avoiding bubbling at all times. Samples were first

† This work has been supported by a research grant from the Sigrid Juselius Foundation. M.I.V. and J.E.M. are recipients of fellowships from the Academy of Finland (M.R.C.).

* Author to whom correspondence should be addressed at the University of Helsinki. On leave from the A. N. Belozersky Institute of Physico-Chemical Biology, Moscow State University, Moscow 119899, Russia.

[1] Abbreviations: *a* minus a_3 spectrum, spectrum reflecting reduction of Fe_a and oxidation of Fe_{a_3} in equal amounts (see Materials a: Methods), produced by subtracting $Fe_{a_3}^{2+}$ minus $Fe_{a_3}^{3+}$ spectrum from Fe_a^{2+} minus Fe_a^{3+} spectrum; E_m, redox midpoint potential (vs normal hydrogen electrode); Fe_a, heme *a* metal center; Fe_{a_3}, heme a_3 metal center; k_f, rate constant of forward process; k_r, rate constant of reverse process; τ, first-order relaxation time constant ($t_{1/e}$).

0006-2960/92/0431-11860$03.00/0

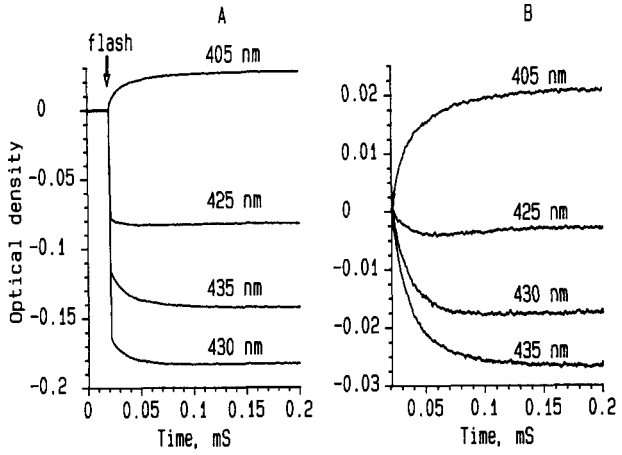

FIGURE 1: Absorption changes after laser photolysis of CO mixed-valence cytochrome *c* oxidase at several wavelengths; panel A presents the complete transient traces, while in panel B the unresolved photolysis component has been subtracted. Enzyme concentration 5 μM; slit width 2 nm; temperature 4 °C (see Materials and Methods).

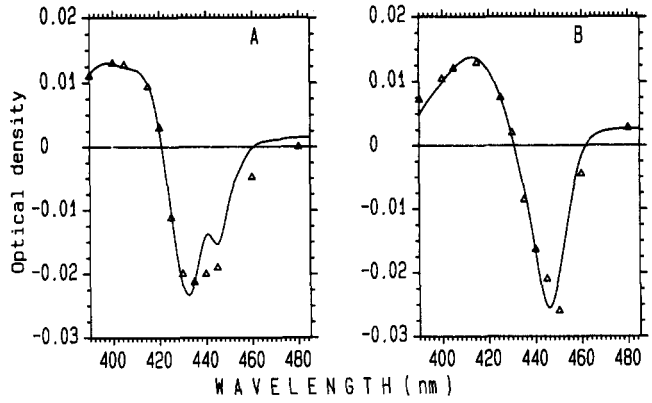

FIGURE 2: (A) Kinetic difference spectrum of the fast (τ = 3 μs) phase (triangles) together with the *a* minus a_3 difference spectrum (solid line). (B) Kinetic difference spectrum of the slow (τ = 35 μs) phase (triangles) together with a spectrum made up of four parts Fe_{a_3} reduced minus oxidized and one part Fe_a reduced minus oxidized spectra. Experimental conditions as in Figure 1.

made anaerobic with several cycles of argon, and then CO was introduced. The two electron-reduced "CO mixed-valence" compound of the enzyme was made by incubating the oxidized enzyme under an anaerobic CO atmosphere for several hours at room temperature [see Bickar et al. (1984)]. Some reduction beyond the two-electron level was usually observed, and the kinetic measurements were made at 4 °C in order to minimize changes in the redox state of Fe_a and Cu_A during experiments.

Transient absorption measurements were made using a single-wavelength spectrophotometer. The probe light source was either a quartz–halogen incandescent lamp or a photographic-type xenon flash lamp. The probe beam was passed through a monochromator before reaching the sample. Photolysis was accomplished by means of a frequency-doubled YAG laser (532 nm; temporal pulse width, 20 ns; pulse energy, 20 mJ), which entered the sample at a right angle to the probe beam. Filters, placed in the probe beam after the sample cuvette, blocked the laser light from entering the photomultiplier tube. Photolysis by the laser was not quantitative, and thus the extent of electron transfer reactions cannot be estimated from the enzyme concentrations alone.

The kinetic spectrum in the near-infrared region was determined as follows: (1) The kinetic traces in this region contain a heme-related component (Boelens et al., 1982). To correct for this, the data at 705 nm, where there should be no contribution from Cu_A, was subtracted from the kinetic data at all other wavelengths. This subtraction was weighted according to the amplitude of the photolysis phase at each wavelength. (2) The amplitude of the slow phase was then taken to be the difference between the absorbance before the flash and that at 400 μs. (No fast phase is visible after the subtraction.)

The "*a* minus a_3" spectrum is a spectrum reflecting reduction of Fe_a and oxidation of Fe_{a_3} in equal amounts. It is obtained by subtracting the $Fe_{a_3}^{2+}$ minus $Fe_{a_3}^{3+}$ spectrum from the Fe_a^{2+} minus Fe_a^{3+} spectrum. These difference spectra were produced by standard ligand-inhibition and subtraction methods [see Vanneste (1966) and Blair et al. (1982)].

RESULTS

Photolysis of the CO mixed-valence compound is followed by multiphasic absorbance changes. Figure 1A shows kinetic traces at several wavelengths in the Soret band superimposed so that the preflash absorbance level is zero in all cases. The fastest component, not resolved in any of the traces, arises from the photolysis of the Fe_{a_3}–CO bond.

In order to focus on the subsequent changes, most of which are related to electron transfer (see below), the same data are shown in Figure 1B but without the fast photolysis component. Two kinetic phases are visible; this is most clear at 425 nm where a fast falling phase is followed by a slower rising phase. At 430 nm, only the faster phase is visible, while at 405 and 435 nm, both phases are seen but they have the same direction. Thus, the fast and slow phases have different spectra, indicating that they are distinct processes. The first phase (τ = 3 μs), was originally observed by Oliveberg and Malmström (1991), who described it as electron flow from Fe_{a_3} to both Fe_a and Cu_B. The slower phase has been assigned as electron transfer from Fe_a to Cu_A (Morgan et al., 1989; Oliveberg & Malmström, 1991).

A rigorous understanding of such processes requires spectra of each kinetic phase. To this end, we constructed kinetic difference spectra, determining the amplitudes of the two phases at each wavelength by a two-exponential fit to the kinetic data.

The Soret spectrum of absorbance changes in the first phase (τ = 3 μs at 25 °C and 7 μs at 4 °C) are shown in Figure 2A (triangles). This kinetic spectrum has a minimum at 435 nm and a broad maximum near 400 nm. The spectrum is not like the reduced-minus-oxidized spectrum of either Fe_a or Fe_{a_3} but is fit quite well by the *difference* between the Fe_a and Fe_{a_3} reduced-minus-oxidized spectra (*a* minus a_3 spectrum, Figure 2A, solid line), as would be expected for electron transfer from Fe_{a_3} to Fe_a.

There is excellent agreement between the stationary and kinetic data below 435 nm, but above this wavelength there are small differences. These discrepancies are apparently due to non-redox-related events (τ = 7 μs) which are also seen after photolysis, in the fully reduced enzyme, where no electron transfer is possible [data not shown; see also Oliveberg and Malmström (1991) and Woodruff et al. (1991)]. These non-redox-related changes have a minimum at 455 nm and a maximum at 436 nm and an amplitude that is very dependent on temperature. At 4 °C (the conditions in Figure 2A) they are relatively small, but at 25 °C they are larger and more dominant in the spectrum. Oliveberg and Malmström (1991) initially described the fast phase as electron transfer from Fe_{a_3} to Fe_a, but on the basis of a discrepancy between their amplitudes at 445 and 605 nm, they suggested that there was also net electron transfer from Fe_{a_3} to Cu_B. Our data suggest

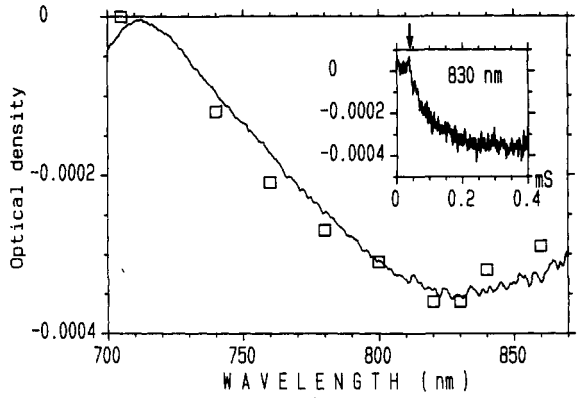

FIGURE 3: Kinetic difference spectrum of absorbance changes in the near-infrared (squares) together with the reduced minus oxidized spectrum (solid line) of the enzyme for the same region (arbitrarily rescaled). The inset shows the kinetic behavior at 830 nm. The arrow indicates the time of the laser flash. All of the kinetic data have been corrected for heme-related absorbance changes, setting the point at 705 nm arbitrarily to zero (see Materials and Methods). Kinetic data: slit width, 20 nm; temperature, 4 °C, enzyme concentration, 5 μM. Static spectrum: buffer, 250 mM sucrose, 100 mM phosphate (pH 7.8), and 0.75% cholate; reductant, dithionite; room temperature.

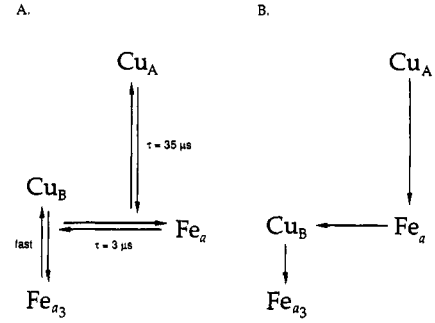

FIGURE 4: (A) Kinetic scheme. (B) Electron pathway scheme (see text).

that this discrepancy can be explained by the non-redox-related absorbance changes. The excellent fit between our kinetic spectrum and the *a* minus and a_3 spectrum at wavelengths below 435 nm, where the effect of non-redox-related changes is minimal, shows clearly that the dominant electron transfer process in the fast phase is electron redistribution from Fe_{a_3} to Fe_a. We also note that the broad absorbance increase near 390 nm in the kinetic spectrum (Figure 2A), which has been assigned to Cu_B^{2+} (Einarsdóttir et al., 1992), is a property of the *a* minus a_3 difference spectrum.

The second phase in the Soret region has a time constant of about 35 μs. A kinetic component with the same rate constant is observed at 830 nm (Figure 3, inset), where Cu_A^{2+} has its absorption band. The kinetic spectrum of this component is shown in Figure 3 (squares), together with the 830-nm band from the (static) reduced-minus-oxidized spectrum (solid line). The similarity of these spectra confirms that the 35-μs phase is due to electron transfer to Cu_A (Boelens et al., 1982).

It appears from the corresponding Soret spectrum (Figure 2B, triangles) that some fraction of both Fe_a and Fe_{a_3} becomes oxidized in this phase. If, as we concluded above, Fe_{a_3} and Fe_a are in fast redox equilibrium on the time scale of the slow phase, then electron transfer from either one of these two hemes to Cu_A will necessarily involve both centers [see Oliveberg and Malmström (1991)]. The (heme) spectrum of this phase would then be expected to be a linear combination of Fe_a and Fe_{a_3} reduced-minus-oxidized spectra, weighted according to the redox equilibrium constant between these two hemes. A good fit to the experimental kinetic spectrum is produced with an equilibrium constant of 4 (Figure 2, solid line), which is equivalent to a difference of 36 mV between the E_m values of Fe_{a_3} and Fe_a (in the relevant states).

DISCUSSION

The construction of kinetic spectra leads to a significant improvement in the analysis of these reactions. The spectra allow us to assign the (thermodynamic) donors and acceptors for both phases of the reaction and calculate the equilibrium constant for the $Fe_a \leftrightarrow Fe_{a_3}$ electron transfer, without relying on absolute amplitudes. This is of special importance since these amplitudes can vary from preparation to preparation. Measurements in submitochondrial particles (not shown) gave significantly larger absolute amplitudes, although the rate constants observed were essentially the same as the ones we have reported. This problem is avoided by the spectral analysis.

Our data are best explained in terms of a cascade of equilibria as shown in Figure 4A. This is a kinetic scheme and does not imply a physical sequence of electron carriers; the electron donor for a given reaction is the system of carriers which equilibrate at faster rates. Thus, the rate of electron exchange between Fe_{a_3} and Cu_B is assumed to be fast relative to the rate of electron transfer from these centers to Fe_a, and the extent to which Fe_{a_3} and Cu_B each becomes oxidized is determined by the difference in their E_m values. Similarly, the electrons which appear at Cu_A during the slow phase come from the (quasi)equilibrium system of Fe_{a_3}, Cu_B, and Fe_a. In the model, any one of the three could be the physical donor to Cu_A. Although this scheme does not require a specific sequence of electron carriers, it is consistent with accepted ideas about pathways of electron flow in cytochrome *c* oxidase (Figure 4B).

The spectrum of the fast phase shows very close to equal amounts of Fe_a becoming reduced and Fe_{a_3} becoming oxidized. This leads to the conclusion that Cu_B does not change its oxidation state in this phase; if Cu_B were to undergo a redox change, there would have to be a corresponding change at either Fe_a or Fe_{a_3}, since Cu_A, the only other possible donor/acceptor, is not in redox equilibrium with these other centers on this time scale (Figure 3, inset). However, in the fast-phase reaction, the same number of electrons arrive at Fe_a as leave Fe_{a_3}, showing that there is neither net reduction (cf. Oliveberg & Malmström, 1991) nor oxidation (cf. Einarsdóttir et al., 1992) of Cu_B. As was noted above, the 390-nm absorbance increase in the fast phase, which Einarsdóttir et al. (1992) assign to Cu_B^{2+}, can be found in the *a* minus a_3 spectrum. This would also appear to be the case with the other feature that these authors assigned to Cu_B^{2+} — a broad band around 520 nm (data not shown). The absence of redox changes at Cu_B after CO photolysis indicates that the E_m of Cu_B is significantly higher than that of Fe_{a_3}, in agreement with redox titration studies, where EPR signals from $Fe_{a_3}^{3+}$, but not Cu_B^{2+}, are observed in partially reduced states of the enzyme [reviewed in Wikström et al. (1981)]. However, our results do not allow us to choose between Fe_{a_3} and Cu_B as the physical electron transfer donor to Fe_a. If, as we have assumed, Fe_{a_3} and Cu_B are in fast redox equilibrium, and the E_m of Cu_B is higher than that of Fe_{a_3}, an electron will appear to come from Fe_{a_3} even if Cu_B is the actual donor.

The slow (35-μs) phase is predominantly electron redistribution from Fe_{a_3} and Fe_a to Cu_A. As described above, the ratio of Fe_a to Fe_{a_3} in the spectrum of this phase allows us to calculate a redox equilibrium constant of 4 between these

centers. From this equilibrium constant and the apparent rate constant observed for the fast phase, we can determine forward and reverse rate constants for electron transfer from Fe_a and Fe_{a_3} as follows: $k_f = 2.4 \times 10^5\ s^{-1}$ and $k_r = 6 \times 10^4\ s^{-1}$.

This forward rate constant is similar to that estimated by Oliveberg and Malmström (1991) solely from the observed rate of the fast phase. As noted by Oliveberg (1992), this is much faster than any observed process in the (flow-flash) reoxidation of the fully reduced enzyme by O_2. It follows that electron transfer per se from Fe_a to the binuclear site is so fast that it can never be significantly rate-determining during catalysis. Woodruff et al. (1991) have shown that the flash-photolyzed CO first binds to Cu_B^+, from which it dissociates in approximately 1–3 μs at room temperature. Einarsdóttir et al. (1992) have suggested that CO dissociation from Cu_B^+ could be a prerequisite for the fast-phase electron transfer, since both events take place on approximately the same time scale. In view of this possibility, our value for k_f must be taken as a lower limit on the true electron transfer rate.

Several workers have shown that, in the reaction of the fully reduced enzyme with O_2, the initial reoxidation of Fe_a takes place with a rate constant of approximately $0.3 \times 10^5\ s^{-1}$ — much slower than k_f — and is simultaneous with the decay of the primary oxy intermediate (Fe_{a_3}–O_2) [for a review, see Babcock and Wikström (1992)]. Hence, oxidation of Fe_a in this reaction must be rate-limited not by the inherent electron transfer rate (k_f) but by another mechanistic step ($k = 0.3 \times 10^5\ s^{-1}$) which follows the oxy intermediate and which limits the observed rate of oxidation of Fe_a. This is consistent with the suggestion (Morgan & Wikström, 1992; Babcock & Wikström, 1992) that the oxy compound is followed by a ferric/cupric peroxy species (P) to which electron transfer subsequently occurs from Fe_a. If compound P is destroyed at a faster rate ($k_f = 2.4 \times 10^5\ s^{-1}$) than it is produced from the oxy compound ($k = 0.3 \times 10^5\ s^{-1}$), it will never be significantly populated. This accounts for the fact that compound P is not observed in flow-flash experiments on the fully reduced enzyme.

The fact that we can now quote a rate constant, k_f, for electron transfer from Fe_a to the binuclear site, as well as a driving force for this reaction, makes it possible to make some structural predictions. Moser et al. (1992a) have demonstrated an amazingly homogeneous dependence of the energy-optimized rate of biological electron transfer processes on the "edge-to-edge" distance between redox centers, which is applicable to a large variety of structurally different biological redox systems. If we assume that the electron transfer from Fe_a to the binuclear site behaves in the same way and that the reorganization energy for this reaction is between 0.7 and 1.0 eV (a range which is typical for biological electron transfers), extrapolating our observed 36-mV driving force to this value (Moser et al., 1992b) yields an energy-optimized rate which corresponds to an "edge-to-edge" distance of 12.0–10.5 Å between the Fe_a heme and the binuclear site electron acceptor. This distance may be compared with a "center-to-center" distance range of 12–16 Å between the hemes (Ohnishi et al., 1982; Mascarenhas et al., 1983; Scholes et al., 1984), subsequently revised by Brudvig et al. (1984) to approximately 20 Å.

ACKNOWLEDGMENT

We thank Alexander Drachev for designing and writing our data acquisition and processing software, Hilkka Vuorenmaa for her excellent technical assistance, and P. L. Dutton for discussions.

REFERENCES

Babcock, G. T., & Wikström, M. (1992) *Nature 356*, 301–309.
Baker, G. M., Noguchi, M., & Palmer, G. (1987) *J. Biol. Chem. 262*, 595–604.
Bickar, D., Bonaventura, C., & Bonaventura, J. (1984) *J. Biol. Chem. 259*, 10777–10783.
Blair, D. F., Bocian, D. F., Babcock, G. T., & Chan, S. I. (1982) *Biochemistry 21*, 6928–6935.
Boelens, R., Wever, R., & van Gelder, B. F. (1982) *Biochim. Biophys. Acta 682*, 264–272.
Brudvig, G. W., Blair, D. F., & Chan, S. I. (1984) *J. Biol. Chem. 259*, 11001–11009.
Brzezinski, P., & Malmström, B. G. (1987) *Biochim. Biophys. Acta 894*, 29–38.
Einarsdóttir, O., Dawes, T. D., & Georgiadis, K. E. (1992) *Proc. Natl. Acad. Sci. U.S.A. 89*, 6934–6937.
Hartzell, C. R., & Beinert, H. (1974) *Biochim. Biophys. Acta 368*, 318–338.
Mascarenhas, R., Wei, Y.-H., Scholes, C. P., & King, T. E. (1983) *J. Biol. Chem. 258*, 5348–5351.
Morgan, J. E., & Wikström, M. (1991) *Biochemistry 30*, 948–958.
Morgan, J. E., Li, P. M., Jang, D.-J., El-Sayed, M. A., & Chan, S. I. (1989) *Biochemistry 28*, 6975–6983.
Moser, C. C., Keske, J. M., Warncke, K., Farid, R. S., & Dutton, P. L. (1992a) *Nature 355*, 796–802.
Moser, C. C., Keske, J. M., Warncke, K., Farid, R. S., & Dutton, P. L. (1992b) *Biochim. Biophys. Acta* (in press).
Ohnishi, T., LoBrutto, R., Salerno, J. C., Bruckner, R. C., & Frey, T. G. (1982) *J. Biol. Chem. 257*, 14821–14825.
Oliveberg, M. (1992) Ph.D. Thesis, Chalmers University of Technology and University of Göteborg, Göteborg, Sweden.
Oliveberg, M., & Malmström, B. G. (1991) *Biochemistry 30*, 7053–7057.
Scholes, C. P., Janakiraman, R., Taylor, H., & King, T. E. (1984) *Biophys. J. 45*, 1027–1030.
Vanneste, W. H. (1966) *Biochemistry 5*, 838–848.
Wikström, M., Krab, K., & Saraste, M. (1981) *Cytochrome oxidase: A synthesis*, Academic Press, London.
Woodruff, W. H., Einarsdóttir, O., Dyer, R. B., Bagley, K. A., Palmer, G., Atherton, S. J., Goldbeck, R. A., Dawes, T. D., & Kliger, D. S. (1991) *Proc. Natl. Acad. Sci. U.S.A. 88*, 2588–2592.

Registry No. Fe, 7439-89-6; Cu, 7440-50-8; cytochrome *c* oxidase, 9001-16-5.